# Magnetic field structures from cosmic-ray driven dynamo

Dominik Wóltański, Michał Hanasz

Centre for Astronomy, Nicolaus Copernicus University, Toruń, Poland

## Abstract

Cosmic-Ray-driven dynamos produce magnetic arms in galactic disks and large-scale helical magnetic fields in galactic halos. Relying on numerical models of hybrid N-body and CR-MHD simulations we show formation of those structures. We discuss the relation of the 3D magnetic field structures with their counterparts in radio maps of synchrotron radio-emission. We suggest that X-shaped structures on polarisation radio-maps of edge-on galaxies result from the projection of large-scale magnetic helices onto the plane of sky.

## Dynamo model

**Spiral galaxy similar to Milky Way:** ⊙ composed of a disk, bulge and halo. Gravitational potential of the galaxy is computed with an N-body algorithm (VINE code [4]). ⊙ Interstellar medium: gas, magnetic field and cosmic rays modelled with the aid of grid-MHD simulations (PIERNIK code [5,6,7,8]). Supernova rate dependent on the local gas density following the Schmidt-Kennicutt law.

**CR-driven dynamo [1,2,3]:** ⊙ Cosmic ray gas described by the diffusion-advection equation, supplemented to the set of resistive MHD equations. CRs diffuse along magnetic field lines. ⊙ Assumed 10% efficiency of CR production in SN remnants, thermal energy output from SNe neglected. ⊙ Finite resistivity of the ISM. ⊙ Differential rotation of the interstellar gas. ⊙ No magnetic field in the initial configuration. Weak, randomly oriented, dipolar magnetic field supplied in 10% of supernova remnants.

## Horizontal disk structure

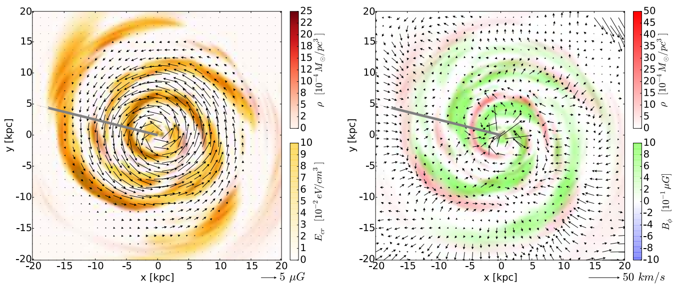

Figure 1: Left panel: 'excess' (over azimuthally averaged distribution) of gas density (red), CR energy density (yelow) and magnetic field (vectors). **Enhanced evergy density of cosmic rays coincides with their production sites – spiral arms.** Right panel: 'excess' of gas density (red), azimuthal magnetic field (green) and nonaxisymmetric component of gas velocity (vectors). **Strong azimuthal magnetic field locates in between gaseous arms.**

## Helical 3D structure of magnetic arms

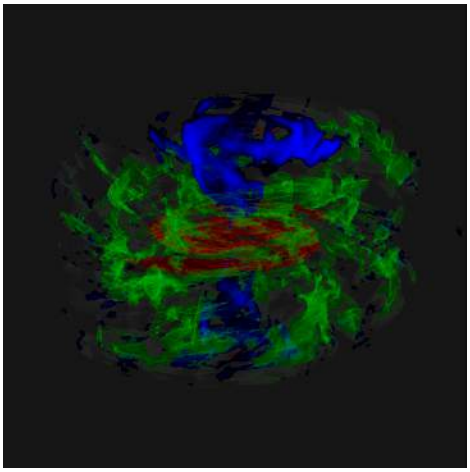

Figure 2: Helical structure of magnetic field surrounding the gaseous disk of spiral galaxy (red). 'Excess' of toroidal magnetic field component $B_\varphi$ above the azimuthaly averaged $\langle B_\varphi \rangle$ is marked green, while 'deficit' ($B_\varphi < 0$) is marked blue. **The large-scale radially-expanding helix forms as the result of wind-advection of the regular magnetic field produced in the disk.**

## Material and magnetic arms

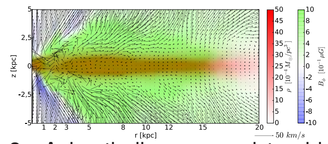

Figure 3: Azimuthally averaged toroidal magnetic field (blue-green) and velocity vectors of the galactic wind.

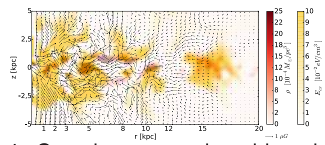

Figure 4: Cosmic rays produced in spiral arms expand in vertical direction.

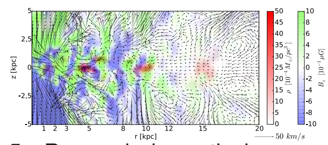

Figure 5: Reversals in vertical magnetic field and buoyancy-driven structures.

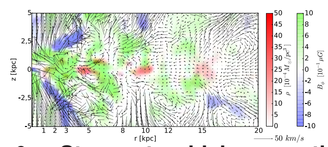

Figure 6: **Strong toroidal magnetic field component (green) located outside gaseous arms.**

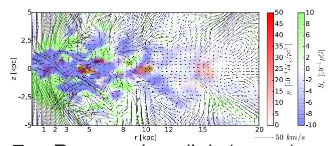

Figure 7: Reversed radial (green) magnetic field component above gaseous arms indicates the effect of Coriolis force twisting of magnetic loops.

## Synthetic radio maps

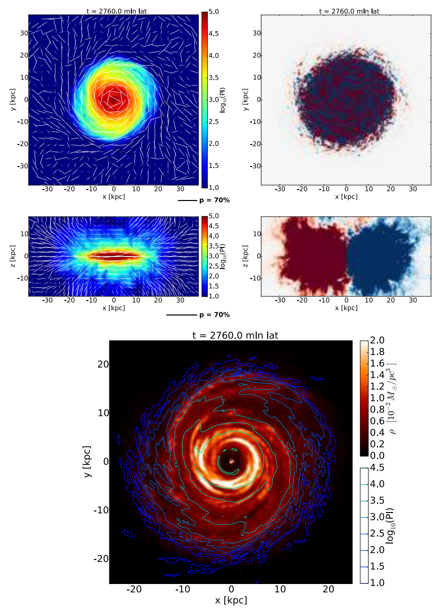

Figure 8: Top-left pair of panels: synthetic radio maps of the polarised intensity and polarisation vectors of synchrotron emision in the edge-on and face-on views. Top-right pair of panels: the corresponding Faraday rotation maps indicating the irregular structure of vertical magnetic field component and coherent toroidal magnetic fields in the large volume occupied by the magnetic helix shown in Figure 2. The lower panel shows contours of polarised intensity superposed onto column gas density map.

## References

[1] Hanasz, M., Kowal, G., Otmianowska-Mazur, K., and Lesch, H. 2004 *2004, ApJ 605, L33*

[2] Hanasz, M., Wóltański, D. and Kowalik, K. 2009 *ApJ. Let. 706, L155*

[3] Kulpa-Dybeł, K., Nowak, N., Otmianowska-Mazur, K., Hanasz, M., Siejkowski, H., Kulesza-Żydzik, B. 2014 *A&A, 575, A93, 2015*

[4] Nelson, A. F., Wetzstein, M. and Naab, T. and . 2009, *ApJ. Supp. 184, 326*

[5] Hanasz, M. and Kowalik, K. and Wóltański, D. and Pawłaszek, R. 2010 *EAS Publ. Series, 42, 275,*

[6] Hanasz, M., Kowalik, K., Wóltański, D., Pawłaszek, R. and Kornet, K. 2010 *EAS Publ. Series, 42, 281,*

[7] Hanasz, M., Kowalik, K., Wóltański, D. and Pawłaszek, R. 2012 *EAS Publ. Series, 56, 363,*

[8] Hanasz, M., Kowalik, K., Wóltański, D. and Pawłaszek, R. 2012 *EAS Publ. Series, 56, 367*

## Acknowledgements

This work was supported in part by Polish Ministry of Science and Higher Education through the grant N N203 511038. The computations have been performed on the GALERA supercomputer in TASK Academic Computer Centre in Gdańsk.